

Effect of Sintering Temperature on Some Physical And Mechanical Properties of Fabricated Hydroxyapatite Used For Hard Tissue Healing

Dr. Kahtan khalaf Al-Khazraji*, Dr. Waleed Asim Hanna**
& Payman Suhbat Ahmed**

Received on:28/10/2008

Accepted on:3/12/2009

Abstract

This work focuses on studying the role of drying and calcination on stiochiometry and crystallinity of deposited HA. Also, studying the effect of sintering temperature on phases generated, physical and mechanical properties of sintered HA powder compact at a range of (800-1200)°C.

Both Ca/P ratio and crystallinity were increased after calcination, where the Ca/P ratio raised from 1.7 to 1.9 and the height of Hydroxyapatite peak intensity was also increased. Secondary phases also appeared.

X-ray diffraction patterns and electrical microscopic pictures of polished surfaces of the Hydroxyapatite compact after sintering had revealed the process of densification and crystallization of Hydroxyapatite. The increase of sintering temperature leads to grain growth, while surface cracking and other defects became lower i.e. porosity and surface voids.

Both hardness and fracture strength were increased for samples sintered at high temperatures where they reached their maximum values at sintering temperature (1200)°C. The maximum linear shrinkage was 20% at sintering temperature 1200°C. The maximum bulk density was (2.173) g/cm³ at sintering temperature of 1200°C and the maximum apparent density was (2.58) g/cm³ at sintering temperature 900°C. The maximum apparent and open porosities were 47.136% and 47.058% respectively at sintering temperature 900°C. The maximum water absorption was 39.13% at sintering temperature 800°C.

Keywords: Bioceramics, preparation of Hydroxyapatite, Bioactive Hydroxyapatite, Reinforcement of Hydroxyapatite.

تأثير درجة حرارة التلبيد على بعض الخصائص الفيزيائية والميكانيكية للهيدروكسي اباتايت المصنع والمستخدم لمعالجة الانسجة الصلبة

الخلاصة

يركز هذا البحث على دراسة دور عمليتي التجفيف و الكلسنة على التوازن الكيميائي و تبلور الهيدروكسي اباتايت المحضر . وكذلك دراسة تأثير درجة حرارة التلبيد على الأطوار المتكونة و الخواص الفيزيائية و الميكانيكية لمسحوق الهيدروكسي اباتايت المكبوس و الملبد ضمن المدى (800-1200)°م.

لوحظ ازدياد كل من التبلورية و نسبة P\Ca بعد عملية الكلسنة , حيث تزداد نسبة P\Ca من 1.7 إلى 1.9 بالإضافة إلى ازدياد ارتفاع شدة قمة الهيدروكسي اباتايت و ظهور الأطوار الثانوية.

* Presidency of University, University of Technology/ Baghdad

** Materials Engineering Department, University of Technology/ Baghdad

أظهرت مخططات الأشعة السينية و صور المجهر الضوئي للسطوح المكبوسة و المصقولة بعد التلييد ، عملية التبلور و التكثف للهيدروكسي اباتايت . أدت الزيادة في درجة حرارة التلييد إلى النمو الحبيبي كما تراجعت الشقوق السطحية و العيوب الأخرى (المسامات والفجوات السطحية). ازداد كل من الصلادة و مقاومة الكسر للنماذج الملبدة في درجات الحرارة العالية حيث تصل إلى أعلى قيمها عند (1200)°م.

أعلى قيمة للتقلص الخطي كانت (20)% عند درجة حرارة تلييد (1200) °م أعلى قيمة للكثافة الكتلية كانت (2.173) غ/سم³ عند درجة حرارة تلييد (1200)°م . أعلى قيمة للكثافة الظاهرية كانت (2.58) غ/سم³ عند درجة حرارة (900) °م وأعلى قيمة للمسامية المفتوحة و الظاهرية كانت (47.058)% و (47.136)% على التوالي عند درجة حرارة تلييد (900) °م ، و أعلى قيمة لأمتصاصية الماء كانت (39.13) % عند درجة حرارة تلييد (800)°م.

1. Introduction

The remarkable progress of ceramics in last decades has resulted in the development of materials with chemical, physical and mechanical properties that are suitable for biomedical application. Ceramic materials used for this purpose are known as bioceramics^[1].

Bioceramics can be used as structural parts like: joint or tissue replacements, can be used as coatings to improve the biocompatibility of metal implants, and can function as resorbable lattices which provide transient structures and a frame work that is dissolved replaced as the body rebuilds tissue. The thermal and chemical stability of ceramics, their high strength, wear resistance and durability all contribute to making ceramics good candidate materials for surgical implants. Some ceramics even feature drug delivery capability^[2, 3].

Calcium phosphate is found in a variety of forms which are well-known in the art, such as hydroxyapatite HA(Ca₁₀(PO₄)₆(OH)₂, Ca/P=1.67) , Tricalcium phosphate

TCP (Ca₃(PO₄)₂, Ca/P=1.5), and brushite (CaHPO₄-2H₂O , Ca/P=1), as well as in amorphous form ACP(Ca_x(PO₄)_y NH₂O, Ca/P= ≈ 1.5). The relative stability of the predominant form of calcium phosphate is ACP<TCP<<HA^[4]. Among calcium phosphate forms: HA, bioactiveglass and glass-ceramic are used in biomedical field^[5].

Among the calcium phosphate ceramics, i.e., Ca₄P₂O₉, HA and TCP(β-whitlockite), are known to lead to differences in biodegradation behavior that biodegradable TCP ceramics give rise to extensive bone remodeling around the implant^[1].

Apatite is one of very few minerals which are produced and used by biological systems^[6].

Apatite is a group of minerals which usually refer to hydroxyapatite , fluoroapatite , and chloroapatite , named for high contaminations of OH⁻ , F⁻ , Cl⁻ ion respectively , in the crystal lattice^[7,8].

HA is the major component of tooth, enamel, and a large component of bone material^[9].

Synthetic carbonate apatites usually display reduced crystallinity whereas biological apatites appear to become more crystalline as the carbonate content increases^[9].

The naturally occurring form of calcium apatite is with the formula $\text{Ca}_5(\text{PO}_4)_3(\text{OH})$, but is usually written $\text{Ca}_{10}(\text{PO}_4)_6(\text{OH})_2$ to denote that the crystal unit cell comprises two molecules. Pure hydroxyl apatite powder is white, odorless and tasteless^[6,10]. Table (1) illustrates the identity of hydroxyapatite^[6,10,11,12,13].

Synthetic hydroxyapatite is of great importance as a biomaterial. It is one of the few materials that are classed as bioactive (it is one of two materials capable of forming a chemical bond with bone. In vivo—the other being bioactive glass of various compositions^[14].) Unlike other materials such as alumina and zirconia, which are identified as foreign materials and become encapsulated by fibrous tissue. HA is sometimes used in powder form, but in most cases it is used as a bulk material^[15].

HA powder is sensitive depending on preparation conditions e.g. the reaction system used, starting material, pH, temperature, ripening time, calcination temperature, etc^[18]. Pore volume and size distribution greatly depends on both sintering temperature and sintering method^[19].

Pure HA degrades rapidly and easily if conditions are correct: pH, chemical attack, phagocytosis^[20].

HA powders have generally been synthesized from aqueous solutions for use in bioceramic applications. It is known that calcium HA is the least

soluble and the most stable compound of calcium phosphate phases in aqueous solutions at pH values higher than 4.2. However; HA powders synthesized in highly alkaline media were recognized by their relatively high thermal stability and phase purity even after high temperature (1100-1300) °C sintering^[21].

Some secondary phases are formed during HA sintering process and there are related to its^[22]:

a-Original Ca/P ratio. b-Chemical composition. c-Sintering temperature

2. Experimental work

The following materials were used for the preparation of HA powder: -Calcium hydroxide $\text{Ca}(\text{OH})_2$, -Phosphoric acid H_3PO_4 , -poly-vinyl alcohol (PVA) as a binder, -drops of sodium hydroxide (NaOH) used as pH fixer^[18], -Distilled water, -Ethanol(99.9%) .

A suspension of (27)g of $\text{Ca}(\text{OH})_2$ was dissolved in 1000ml of distilled water and vigorously stirred, then a solution of (24.6)g of H_3PO_4 was diluted in 1000ml of distilled water was slowly added as dropwise over 1 to 2hrs under a condition of pH=8 to produce a gelatinous precipitate .

The reaction mixture was aged at room temperature for a week. The resulting slurry was cleared by removing floated liquid and then washed with distilled water followed by clearing from floating liquid and then washed with ethanol and the floated liquid was also cleared.

The resulting slurry was dried at 80°C in an oven over night; the resulting material was re-milled and calcined at 800°C for 3hrs.

The finely ground powder was mixed with 2% PVA and 250ml warm distilled water and mixed for 15 mins, and then dried in an oven at 80°C and then the re-milled powder was sieved to (<106µm)^[23,24].

Pressing was done by a hydraulic pressing machine with capacity of (384.31)Mpa in a tool steel die of (2.55cm) in diameter with pressing pressure of (76.756) Mpa for two minutes.

Sintering of samples were done at different temperatures of (800, 900, 1000, 1100, 1200) °C and at holding time of (3) hrs. With a heating rate of 5°C/min^[9] is set up to the required temperatures, then left in the furnace for cooling.

Characterization of sintered samples

X-ray diffraction inspection was performed by using Philips diffract meter pw 1840 with a Cu K α radiator tube and Ni filter and the diffraction angle (2 Θ) was between (20-60)°.

And Ca/P ratio for the HA powder was evaluated before and after calcinations by atomic absorption and the ratio was 1.7 before sintering and 1.9 after sintering.

Electron microscopic examination was used to evaluate the particle shape .Figure (1) shows the particle shape of HA powder which obviously seems irregular and semicircular with a wide distribution .And Particle size distribution was carried out in a laser diffraction particle size analyzer “SHIMADZU SALD-2101”, The mean value of diameter was (87.821)µm and the median value was (123.483)µm.

Apparent and real densities were measured by the conventional methods i.e. cup cone and pycnometer respectively^[25,26].

Sintered samples were prepared by grinding and polishing then etched with (0.1)M of acetic acid CH₃COOH , followed by washing with distilled water then with ethanol . And the sample surfaces were colored with ink to enhance the microstructural observation which was examined by an optical microscope at a magnification of (X 63).

Linear shrinkage percentage was measured depending on diametral change by using micrometer, before and after sintering

$$\text{Linear shrinkage \%} = \frac{D_o - D}{D} * 100$$

L.sh: Linear shrinkage.

D_o : Sample diameter after pressing (mm).

D : Sample diameter after sintering (mm).

Apparent and bulk densities as well as apparent and open porosities of sintered HA compact powder were measured, using the standard Archimede's method^[25,26] .

Fracture strength test was carried out by using the diametral compression disc test (Brazilian test) where the disc was placed between two surfaces and a load was applied in the rate of (0.5 mm/min) , then the force obtained at fracture was recorded , then the following equation was applied to calculate the strength of material^[29]:-

$$\sigma_f = \frac{2p}{\pi dt}$$

σ_f :fracture strength (N/mm²).

P : applied load (N).
 d :sample diameter (mm).
 t :sample thickness (mm).

Vickres method was used to measure the hardness of the sintered samples at loading force of (5N) then using the following equation:-

$$HV = 1.8544 \frac{P}{(d_{av})^2}$$

P : applied load (kg)
 d_{av} : indentation of average diameter (mm)

HV : hardness value (kg/mm²)

3.Results and Discussion

Both Ca/P ratio and crystallinity were increased after calcination, where the Ca/P ratio was increased from 1.7 to 1.9 and the height of (HA) peak intensity was also increased. Secondary phases appeared i.e.(β - $Ca_3(PO_4)_2$, $Ca_2P_2O_7$, β - $Ca_2P_2O_7$, $Ca_4P_2O_9$), according to the X-ray diffraction patterns as explained in appendix (1a,b).The existense of secondary phases such as $Ca_2P_2O_7$ and $Ca_3(PO_4)_2$ associated with (HA) will enhance the biological activity of (HA) .The increase in Ca/P ratio is due to the appropriate pH and calcination temperature which leads to more easily increase of Ca/P ratio up to about 1.9 .Such increases in Ca/P ratio may be related to ease of release of $(PO_4)^{3-}$ ions from the solid phase to the liquid phase at high pH and high temperature^[18] .

HA phase was the major phase at almost X-ray patterns reflections, also $Ca_2P_2O_7$ is observed at many X-ray diffraction patterns. Other secondary phases indicated were α - $Ca_2P_2O_7$, β - $Ca_2P_2O_7$, γ - $Ca_2P_2O_7$, δ - CaP_2O_6 , $Ca(PO_3)_2$, $Ca_3(PO_4)_2$, β -

(CaP_2O_6) and $Ca_4P_2O_9$.(EM) pictures of polished surfaces of the sintered HA powder compacts after sintering revealed the process of densification and crystallization of HA , They were used to evaluate the surface defects (cracks and pores) that could be formed in HA samples during sintering with the varying of sintering temperature.

It can be seen in appendix (2 a-e) that intensity peak heights of HA vary with the increase of temperature , and it reaches the maximum height at 900°C, then decreases at 1000°C to increase again at 1100°C and decreases again at 1200°C. The decrease of the peak heights is due to the formation of different phases .The increase of temperature leads to grain growth at which the maximum grain size can be observed at 1200°C. It also seems that at 1200°C the surface crack and other defects become lower, as shown in figure (2,e).

As temperature of sintering increases the linear shrinkage increases because of the evaporation of binder, moisture and the densification^[31].The maximum linear shrinkage was 20% at 1200°C and the minimum L.sh % was 0.67% at 800°C. The linear shrinkage percentage increases with the increase of temperature because of surface area of fine particles that have their effect on components. After firing, surface area is much reduced^[32].Linear shrinkage behavior with temperature is shown in figure (3).

Apparent density and bulk density relatively increase with the increase of temperature as shown in figure (4, 5), because of the increase of water loss

and linear shrinkage due to densification and the differences between densities are affected by chemical composition^[33]. Particle size and shape of particles of powder which is varying from semicircular to irregular shapes with different size distribution of small particles. It is obvious that at temperature of 900°C the apparent density is increased due to the wide presence of (HA, $D_x=3.156$) depending on the heights of peak intensities and (β - $\text{Ca}_2\text{P}_2\text{O}_7$, $D_x=3.128$) and ($\text{Ca}_2\text{P}_2\text{O}_7$, $D_x=3.09$) which have high densities compared with the other phases in 800°C and 1000°C. It seems that the appearance of ($\text{Ca}_3(\text{PO}_4)_2$, $D_x=2.87$) phase at these temperatures is the reason for being that apparent density lower at 900°C, and both densities (apparent and bulk) increase again after 1000°C due to the presence of (HA) and β - $\text{Ca}_2\text{P}_2\text{O}_7$ in high intensities. The maximum bulk density was (2.173) g/cm^3 at 1200°C and the maximum apparent density was (2.58) g/cm^3 at 900°C. The minimum bulk density was (1.2) g/cm^3 at 800°C and the minimum apparent density was (2.27) g/cm^3 at 800°C.

Apparent and open porosities are decreased with increasing temperature as shown in figure (6,7) due to the reduction in pore volume and the total volume of the sintered compact powder because of the increase in density^[34], while the (OH) as a vapor phase released from (HA) could represent the major reason that caused the remaining micro pores^[32]. The maximum apparent and open porosities were 47.136% and 47.058% respectively at 900°C and the

minimum apparent and open porosities were 12.379% and 12.57% at 1200°C. Water absorption decreases with the increase of sintering temperature as shown in figure (8) since the water absorption is proportional to apparent porosity^[31]. The maximum water absorption was 39.13% at 800°C and the minimum water absorption was 5.785% at 1200°C.

At low temperatures fracture strength is relatively high as temperature increases the fracture strength decreases and it reaches its minimum amount (1.15) N/mm^2 at (1000) °C as shown in figure (9) i.e. fracture at this regime is brittle and occurs by extension of inherent flaws, at all intermediate temperature regime, the strength falls because the formation of low strength phases (β - $\text{Ca}_2\text{P}_2\text{O}_7$, γ - $\text{Ca}_2\text{P}_2\text{O}_7$ and $\text{Ca}_3(\text{PO}_4)_2$), and the fracture occurs from flaws now produced by limited plastic flow. At high temperatures regime where the strength raises again with temperature increase until it reaches its maximum value (6.57) N/mm^2 at 1200°C due to the increase in mechanical bonding^[34] and fracture at this regime is accompanied by extensive plastic deformation^[35].

Hardness increases slightly at low temperatures and then decreases at 1000°C, then it starts increasing at higher temperatures as shown in figure (10). The maximum hardness was (87.4) Kg/mm^2 at 1200°C and the minimum hardness was (36.2) Kg/mm^2 at 1000°C. The slight increase in hardness in the first stages of sintering is due to the formation of grain boundaries by atomic diffusion

in solid state sintering process. The decrease in hardness may be attributed to the formation of multi-phases which comprise different thermal expansion coefficient, which may exhibit cracking near to grain boundary phases^[31]. Hardness increases again due to the decrease in porosity and due to the fracture of the walls between contiguous pores which is lower at high temperatures^[36].

4. Conclusions

1-At 1000°C, a critical point exists in most of the physical and mechanical properties due to the formation of multiple phases.

2-1200°C, is preferred to get high fracture strength and hardness, where the fracture strength was (6.57) N/mm² and the hardness was (87.4) Kg/mm².

References

[1] Czernuszku, J. "Biomaterials under the microscope" Materials world, vol.4, Pp.(452-53) <http://www.azom.com/oars.asp> retrieved at January 2005.

[2] Heness G., Nissan B. Ben "Biomaterials-classifications and behavior of different types of biomaterials" Materials Forum, vol.27 <http://www.azom.com/oars.asp>, retrieved at may 2006.

[3] Sigma Aldrich "ceramic and metal biomaterials applications and types of metal and ceramic biomaterials" <http://www.azom.com/oars.asp> retrieved at march 2006.

[4] Marra, K.G. and Spitzer, R.S.: "Method of manufacturing Hydroxyapatite and uses there for in delivery of nucleic acids". J. Biomaterial res. Mar 15, vol.4, no.59, p.p.(690-696) (2002).

[5] Salame Khalil, Ouaknine Georges E.R., Razon Nissim and Rochkind Simion: **(The use of carbon fiber gates in anterior cervical antibody fusion)**, neuro surg focus, vol.12, no.1, (2002).

[6] Wopenka, Pasteris J.D. "Hydroxyapatite" Materials science and engineering J., vol.2, No.2, Pp.131 <http://en.wikipedia.org/wiki/> retrieved at January 2005.

[7] www.icsucope.org/downloadpubs/scope54/frossard.htm retrieved at march 2006

[8] Seaman John C., Arey J. Samuel and Bertsch Paul M.: **Immobilization of nickel and other metals in contaminated sediments by Hydroxyapatite addition** Journal of environmental quality 30, p.p.(460-469), (2001).

[9] Rajewski A.K., Ravaglioli A., Roveri N., Bigi A. and Foresti E.: **Effect of fluoride, chloride and carbonate ions introduced by cyclic PH fluctuation on the physico-chemical properties of apatite based ceramics** J. of materials science, vol.25 No.7, July p.p.(3203-3207), (1990).

[10] Lewis Richard S., Reinhold van Nostrand " **calcium hydroxyapatite**" [www.mfa.org/ CA MEO/Frontend/materialdescription.asp?name](http://www.mfa.org/CA_MEO/Frontend/materialdescription.asp?name) retrieved at June 2006.

[11] Murugan R. and Ramakrishna S.: **Crystallographic study of Hydroxyapatite bioceramics derived from various sources, crystal growth and design**, vol.5, no.1, September (2004).

[12] Gerd Willman: **Coating of implants with Hydroxyapatite material connection between bone**

and metal advanced engineering materials, vol.7, no.2, p.p.(95-105), (1999).

[13] Limin Sun, Berndt Christopher C., Karlis A. Gross and Kucuk Ahmet: **Material fundamentals and clinical performance of plasma sprayed Hydroxyapatite coating: a review** J. Biomed Mater Res, vol.58, p.p.(570-592), (2001).

[14] Ruys A.J.: **A feasibility study of silicon doping of Hydroxylapatite**, *interceram* vol.42, no.6, p.p.(373-374), (1993).

[15] Chai Cameron, Nissan Besim Ben " **Hydroxyapatite-Thermal stability of synthetic Hydroxyapatite**" International ceramic monograph, vol.1, No.1, Pp.(79-85) <http://www.azom.com/oars.asp>, retrieved at July 2005.

[16] Foppiano Slivia, Marshal Salley J., Marshal Grayson W., Saiz Eduardo and Tomsia Antonio P.: **The influence of novel bioactive glasses on in vitro osteoblast behavior** J. Biomed. Mater. Res. 71A, p.p.242-249), (2004).

[17] <http://www.mivtherapeutic.com> retrieved at March 2006.

[18] Monma H. and Kamiya T.: **Preparation of Hydroxyapatite by the hydrolysis of brushite**. Journal of material science vol.22, no.12, December p.p.(4247-4250), (1987).

[19] Kokubo T.: **Novel ceramics for biomedical applications**. J. Aust. ceram. soc./vol.36 /no.1, p.p.(47-52), (2000).

[20] <http://www.latch.edu/tech/engr/bme/galeclasses/biomaterials/17othe rmats.pdf> retrieved at February 2005.

[21] Bayraktar Defne and Cunet Tas A.: **Chemical preparation of carbonated calcium Hydroxyapatite powders at 37° c in Urea-containing synthetic body fluids**. Journal of European ceramic society, vol.19, p.p.(2573-2579), (1999).

[22] Rodrigus, C.V.M.; Serricella, P.; Farina, M: **Effect of sintering process on morphological properties of bovine bone Hydroxyapatite**. XIX congress of the Brazilian society for microscopica, vol.12, supplement c, September p.p.(37-38) ., (2003).

[23] Gross K. A. and Berndt C.C: **Optimization of spraying parameters for Hydroxyapatite**, 2ND plasma-Technik-symposium, vol.3 p.p.(159-170) ., (1990).

[24] Akao, M. Aoki, H. Kato K.: **Mechanical properties of sintered Hydroxyapatite for prosthetic application** vol.16, no.3, March p.p.(809-812), (1981).

[25] ASTM, "Annual Book of ASTM Standards section (10); Electrical Insulation and Electrons", vol.(15.05), (1988).

[26] Singer, F. and Singer, S.S. "Industrial Ceramics", Shpan and hall Ltd, London, (1963).

[27] Griffiths, R. and Radford, C. "Calculation Ceramic", Macharen and sors Ltd, London, (1964).

[28] Obaid, Inaam.M.Al., "Physical and Mechanical Properties of Alumina compact", M.Sc. Thesis, University of technology, Applied Science. Dep, (1999).

[29] F.A. Chyad, "The effect of metastable Zirconia on the properties of opc

composite", Ph.D. Theses, University of Bradford U.k.(1989).
 [30] Lakhtin, Y., "Engineering Physical Metallurgy", published by Mir publishers, Moscow, (1977).
 [31] Al-Nasir, Waleed Asim " Study the effect of TiO₂ addition on some of the physical and mechanical properties of (Na₂O-CaO-SiO₂-P₂O₅) system" Ph.D, university of technology, Iraq, (2002).
 [32] Abdurassol, Ali Hammode (2005): Assessment of the utilization of hussainiyat bauxite and akashat phosphorite in preparing bioceramic material .PH.D ,University of Baghdad ,Iraq .
 [33] بيداء حسن وحيد: دراسة تأثير إضافة الزركونيا المثبتة جزئياً ZrO₂-Y₂O₃ في بعض

الخصائص الفيزيائية و الميكانيكية للنظام (Na₂O-CaO-SiO₂-P₂O₅) رسـالة ماجستير، الجامعة التكنولوجية، العراق (2006).
 [34] أ.د. الخزرجي، قحطان "ميتالورجيا المساحيق"، وزارة التعليم العالي و البحث العلمي جامعة بابل-كلية الهندسة. قسم هندسة المواد (1997).
 [35] J.C.Knight and T.F.Page: Mechanical properties of highly porous ceramics part I: Modulus of rapture and fracture toughness .ceram. Trans. J., vol.85, no.7, p.p.(27-35) , (1986).
 [36] Boch ,P. and Glandus ,J.C.: Porosity effects on mechanical properties of ceramics .Inter. ceram.J.June, vol.32, no.3, (1983).

Table (1) illustrates the identity of hydroxyapatite.

Chemical formula	Ca ₁₀ (PO ₄) ₆ (OH) ₂	Hazard and safety	Non flammable
Abbreviation	HA	Solubility	Soluble in mineral acid
Melting point(°C)	1670	Insolubility	Insoluble in water, ethanol, acetic acid.
Molecular weight	Mol. Wt=1004.69	Porosity	Open, interconnective.
density	3.08-3.18	Clinical results	Available from 10 years of application.
Ca/P	1.67	Mineral phase	CaO<1% , TCP<1%
Mohs hardness	5	Implant bone connection	Enabling the stablishment of positive material connection.
Refractive index	1.63	biocompatibility	Bioactive, osteoconductive .
Solubility constant K _s at 25 °C	6.62*10 ⁻¹²⁶	Crystal structure	Hexagonal a=b=9.432, c=6.881
synonyms	Tricalcium phosphate, tricalcium orthophosphate tribasic calcium phosphate, bone ash.		

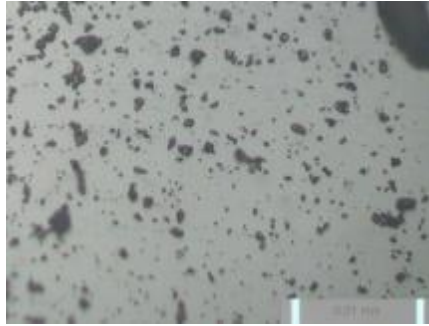
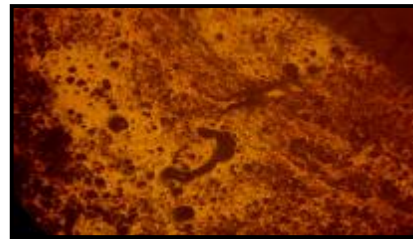
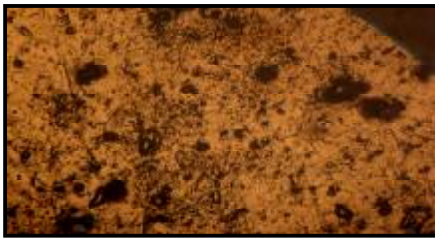


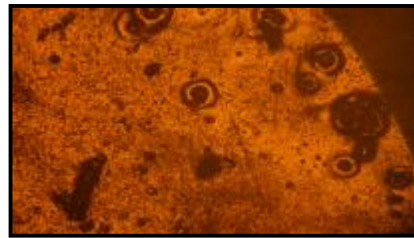
Figure (1) shows the particle shape of fabricated HA



b. 900°C



c. 1000°C



d. 1100°C

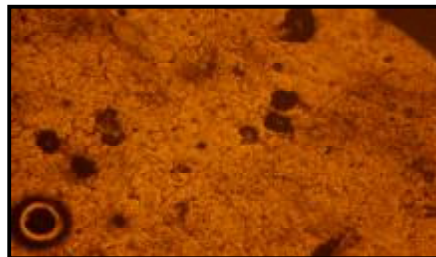


Figure (2) EM pictures of sintered HA powder compact at different Sintering temperatures and at a magnification of (X63) .

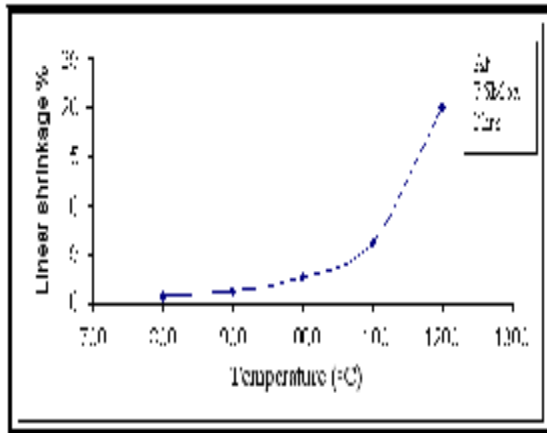


Figure (3) shows the effect of sintering temperature on linear shrinkage of sintered (HA) powder compact

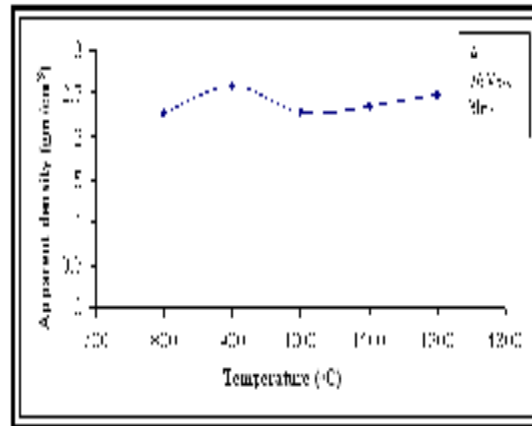


Figure (4) shows the effect of sintering temperature on apparent density

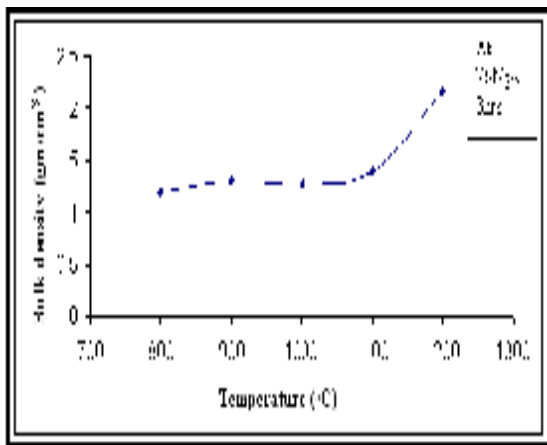


Figure (5) shows the effect of sintering temperature on Bulk density of sintered (HA) powder compact.

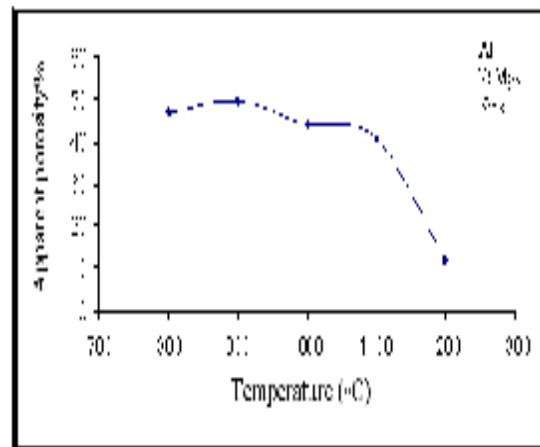


Figure (6) shows the effect of sintering temperature on apparent porosity% of sintered (HA) powder compact.

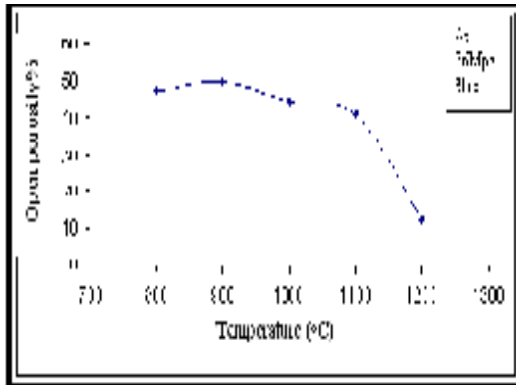


Figure (7) shows the effect of sintering temperature On open porosity% of sintered (HA) powder compact.

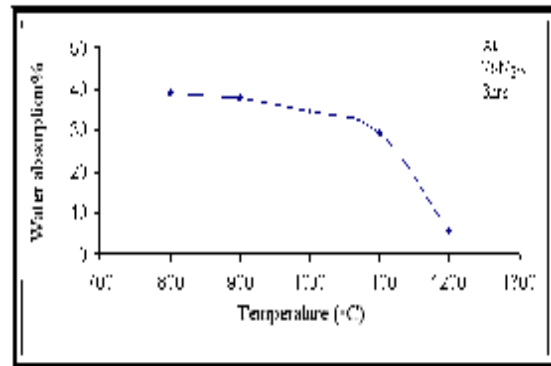


Figure (8) shows the effect of sintering temperature on water absorption of sintered (HA) powder compact.

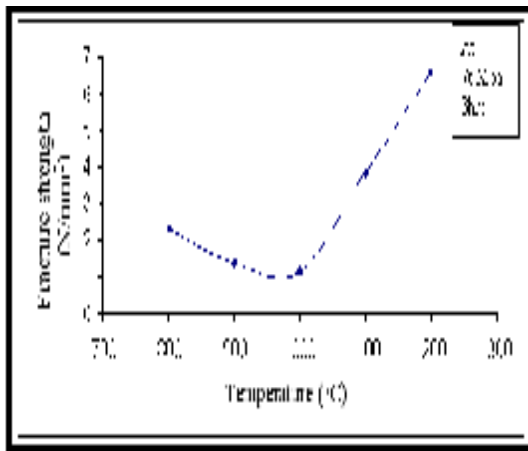


Figure (9) shows the effect of sintering temperature or Fracture strength of sintered (HA) powder compact.

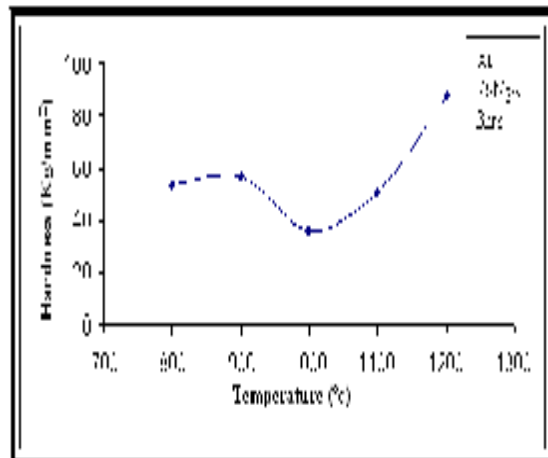
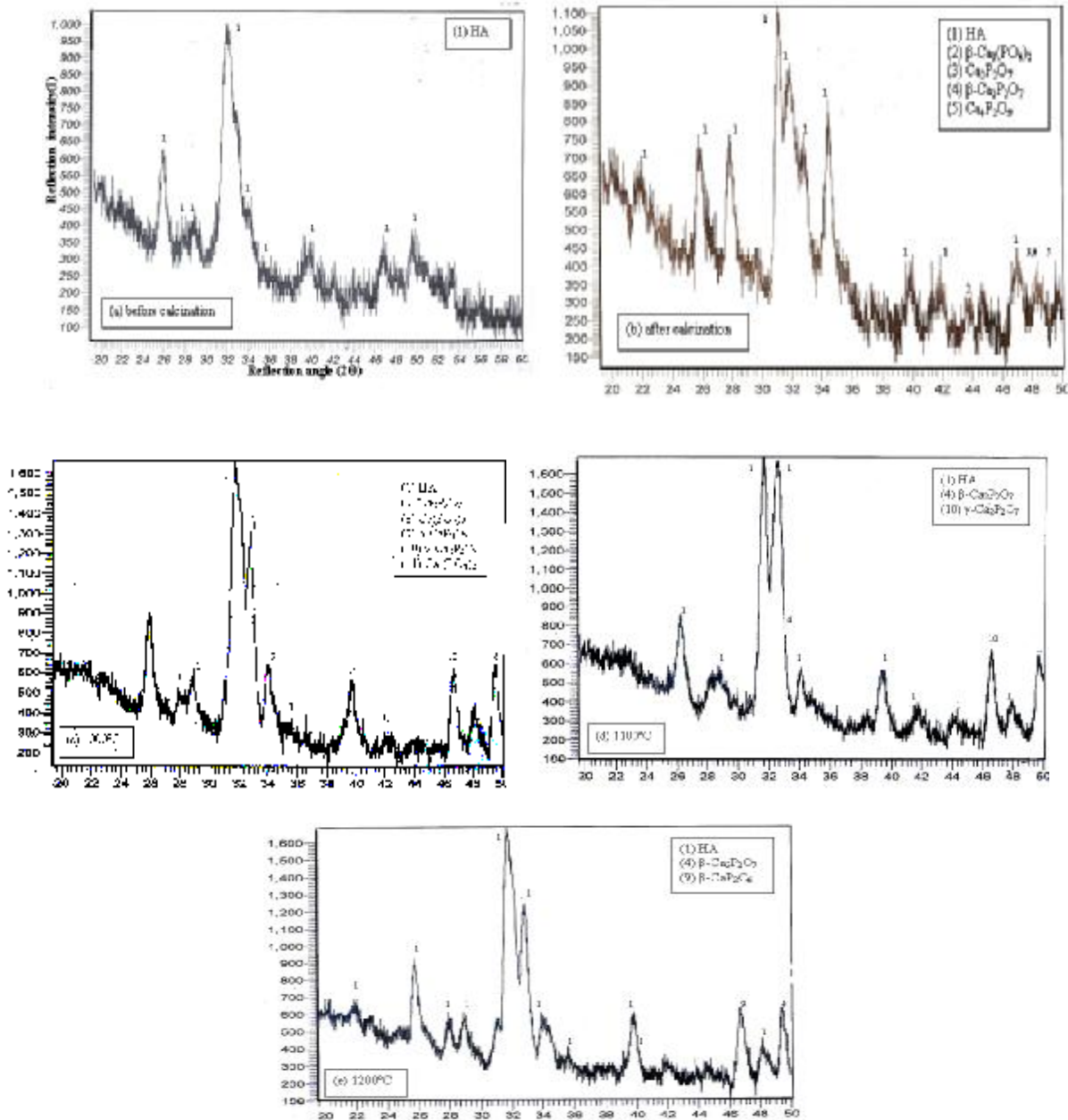


Figure (10) shows the effect of sintering temperature or Hardness of sintered (HA) powder compact.



Appendix (2-a to e) shows x-ray patterns for Hydroxyapatite powder compact samples at temperature range (800-1200)°C .